THE USE OF CHARGE COUPLED DEVICES IN ELECTROOPTICAL PROCESSING

M. A. Monahan, R. P. Bocker, K. Bromley, A. C. H. Louie,
R. D. Martin, and R. G. Shepard

U.S. Naval Electronics Laboratory Center
Electrooptics and Optics Division
San Diego, California

ABSTRACT. The use of coherent optical analog methods to perform matrix multiplications has been reported in the literature. Described in this paper are two incoherent optical systems in which the matrix multiplication represents a general linear transformation of one data vector into another. The input data vector is represented as a time sequence of N amplitude weighted electrical pulses which temporally modulate the light output of an LED. This modulated light field first passes through optical transparency and is then incident upon a charge coupled device (CCD). In one system the CCD is a 500 x 1 element line array and in the other it is a 100 x 100 area array. The transparency is arranged in a rectangular array of M x N elements, where the transmittance of each element is proportional to the m, n^{th} sample of the impulse response or kernel of the linear transformation. Finally, the output data vector is in the form of a time sequence of M electrical pulses, the amplitudes of which represent the values of the desired output data vector.

The linear transformation thus performed is one of broad application, the particular nature of the transformation depending upon the form of the impulse response encoded into the optical memory transparency. Examples of transformations which can be readily programmed into the device include convolutions; correlations; Fourier, Laplace, and Walsh-Hadamard transformations; and linear filtering.

An electrooptical system is particularly appropriate for such calculations in moderate-accuracy (6-8 bit) applications. A direct evaluation of this discrete matrix operation requires M x N analog multiplications to be performed in a sequential manner such that the elements of the output vector are produced one at a time. To significantly reduce the processing time relative to such a slow direct implementation, one must reduce the time required for each analog multiplication, process in parallel, or both. In the electrooptical systems described here, both of these processing advantages are inherently present.

INTRODUCTION

The use of coherent optical analog methods to perform matrix multiplications has been reported in the literature.[1-3] An electrooptical approach utilizing incoherent optical technology has recently been described in which a vidicon tube was used as the integrating element.[4-6] Presented below is an extension of this latter work in which the vidicon is replaced by a line-array charge coupled device (CCD) in one system, and by an area-array CCD in another.[7, 8]

We consider the electrooptical implementation of a general linear filter, illustrated in Fig. 1, which is characterized by an impulse response h(u;v). The output of such a filter, g(v), is related to the input, f(u), through a general linear transformation

$$\int_{-\infty}^{\infty} f(u)h(u;v)du = g(v) \qquad (1)$$

in which the impulse response appears as a weighting function. We shall not restrict our discussion to shift-invariant filters, for which Eq. (1) would reduce to a simple convolution, and will therefore be able to treat a larger class of useful linear transformations. The relation described by Eq. (1) is one of broad application, the particular nature of the transformation depending on the form of the impulse response. Table 1 lists a few examples of signal processing transformations together with the appropriate form of h(u,v). Thus, a signal processing device for which the impulse response can be readily programmed, and which can subsequently perform the transformation of Eq. (1) with economy

of time and hardware, should find widespread and versatile use.

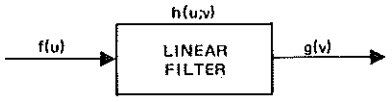

Fig. 1. General linear filter characterized by impulse h(u;v). Input f(u) is transformed into output g(v) through a linear transformation integral.

TABLE 1. EXAMPLES OF LINEAR TRANSFORMATIONS COMMONLY USED IN SIGNAL PROCESSING APPLICATIONS. EACH TRANSFORMATION IS OF THE FORM OF EQ. (1), WITH IMPULSE RESPONSE h(u;v) AS SHOWN BELOW.

TRANSFORMATION	IMPULSE RESPONSE
Convolution	h (v-u)
Cross correlation	h (u-v)
Autocorrelation	f (u-v)
Cosine transform	cos (2πuv)
Fourier transform	exp (-i2πuv)
Laplace transform	exp (-uv)
Hankel transform	$2\pi J_o(2\pi uv)u$

Anticipating the electrooptical implementations to be described below, which are basically sampled data systems, we consider the discrete finite version of Eq. (1).

$$\sum_{n=0}^{N-1} f_n h_{mn} = g_m \qquad m = 0,1,2,\ldots,M-1 \qquad (2)$$

It is often useful to rewrite this equation in its equivalent matrix notation

$$[H]\,[F] = [G].$$

Written in full this relation becomes

$$\begin{bmatrix} h_{00} & h_{01} & \cdots & h_{0,N-1} \\ h_{10} & h_{11} & \cdots & \cdot \\ \cdot & \cdot & & \cdot \\ \cdot & \cdot & & \cdot \\ \cdot & \cdot & & \cdot \\ \cdot & \cdot & & \cdot \\ h_{M-1,0} & & \cdots & h_{M-1,N-1} \end{bmatrix} \begin{bmatrix} f_0 \\ f_1 \\ \cdot \\ \cdot \\ \cdot \\ \cdot \\ f_{N-1} \end{bmatrix} = \begin{bmatrix} f_0h_{00}+f_1h_{01}+\cdots+f_{N-1}h_{0,N-1} \\ f_0h_{10}+f_1h_{11}+\cdots+f_{N-1}h_{1,N-1} \\ \cdot \\ \cdot \\ \cdot \\ \cdot \\ f_0h_{M-1,0}+f_1h_{M-1,1}+f_{N-1}h_{M-1,N-1} \end{bmatrix} = \begin{bmatrix} g_0 \\ g_1 \\ \cdot \\ \cdot \\ \cdot \\ \cdot \\ g_{M-1} \end{bmatrix} \qquad (3)$$

where each matrix has a direct interpretation in terms of the processors described in this paper.

At this point, it is appropriate to comment on why an electrooptical implementation of this fundamental matrix operation is being considered here. Note that a direct evaluation of Eq. (3) requires M x N analog multiplications to be performed in a sequential manner such that output values g_m are produced one at a time. In order to increase the rather slow processing rate associated with such a direct approach, one must reduce the time required for each multiplication, process in parallel, or both. In an optical system both of these processing advantages are inherently present. Although they must still be detected, analog multiplications take place as fast as light travels through an optical transparency (about 10^{-13} sec). Also, the two-dimensional nature of image transfer in an optical system provides the capability of performing many such multiplications simultaneously (up to about 10^6 in the systems described below). Therefore, in applications involving high-speed calculations of moderate accuracy (6–8 bit), an electrooptical system seems a particularly appropriate approach.

We describe in sections to follow two different electrooptical devices designed to implement the matrix multiply operation of Eq. (3). The first utilizes a scanning mirror to sweep the temporally modulated image of an optical memory transparency or mask across a line-array CCD. The second eliminates the need for a scanning mirror by replacing the line-array detector with an area-array CCD and electronically scanning the mask image within the detector itself.

LINE-ARRAY PROCESSOR

GENERAL DESCRIPTION

Fig. 2 depicts the incoherent electrooptical system used to evaluate the matrix multiplication of Eq. (3). The system consists of: (a) light emitting diode (LED), (b) condensing lens, (c) optical memory mask, (d) imaging lens, (e) scanning mirror, and (f) line-array CCD.

Given a temporal signal f(t), for which some linear transformation must be performed according to Eq. (1), the input to the device is a time sequence of electrical pulses, f_n, which represent sampled values of f(t). These samples are proportional to the elements of the column vector [F] in Eq. (3), and appear as an intensity modulation of the LED. The condensing lens is chosen for uniformity of illumination upon the mask and to maximize the light throughput in the system by imaging the light source into the entrance pupil of the imaging lens. Directly behind the condenser is placed the optical mask in which is encoded the matrix operator

[H]. An image of the mask is then formed by the imaging lens, via a scanning mirror, on the face of the CCD. The scanning mirror is galvanometer driven in a sawtooth fashion such that an image of the mask is repetitively swept across the CCD face at a constant velocity in a direction perpendicular to the long dimension of the array. The CCD is then allowed to integrate the light falling on it during a single passage of the image, and a new output vector [G] is generated and clocked out of the CCD at the end of each minor sweep.

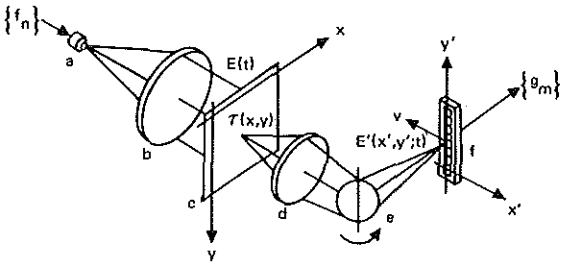

Figure 2. Incoherent electrooptical processor utilizing a mirror scan and line-array CCD. Components are: (a) light emitting diode (LED); (b) condensing lens; (c) optical memory mask; (d) imaging lens; (e) scanning mirror; and (f) line-array charge coupled device (CCD).

MATHEMATICAL ANALYSIS

Given that an analog temporal signal f(t) must be sampled and then transformed according to Eq. (2) into a new discrete signal, we shall proceed by tracing f(t) through the system from input to output. The first step in preparing the analog input signal for processing is to convert it to a time sequence of pulses by passing it through a form of sample-and-hold circuit. The discrete version of the signal, shown in Fig. 3, then becomes

$$f_s(t) = \sum_{n=0}^{N-1} f_n \, \text{rect}\left(\frac{t-nT-d/2}{d}\right) \qquad (4)$$

where

$$f_n \triangleq f(nT)$$

and T is the sampling period, d is the constant pulse duration, and the rectangle function (rect) is defined in Appendix A. The discrete signal $f_s(t)$ is then used to modulate the light emitted by the LED so that the spatially uniform irradiance distribution incident on the optical memory mask in the x,y plane is

$$E(t) = c_1 f_s(t) \qquad (5)$$

where the constant c_1 is a scaling factor which depends on the design of the condensing optics and on the scale of the electrical-to-optical pulse conversion by the LED and its electronics.

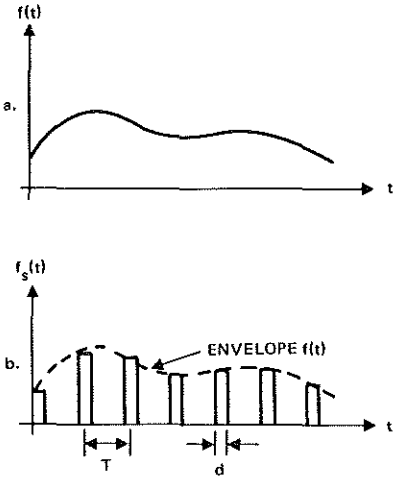

Fig. 3. The input signal (a) and its sampled version (b). Sample pulses of height $f_n \triangleq f(nT)$ and period T are all of same duration d.

The mask itself consists of a total of M x N rectangular apertures arranged in a rectangular array as shown in Fig. 4. Note that each element is the same size, A x B, but that the clear area of each element, a_{mk} x W, is modulated by varying the x-dimension while holding the y-dimension fixed. This design, which modifies the transmitted radiant flux by varying the area of an aperture, is considerably easier to fabricate than one which varies the transmission properties of some photographic or electrooptic material. From the diagram, then, the transmittance function of the optical mask is given by

$$\tau(x, y) = \sum_{m=0}^{M-1} \sum_{k=0}^{N-1} \text{rect}\left(\frac{x-kA}{a_{mk}}\right) \text{rect}\left(\frac{y-mB}{W}\right) \qquad (6)$$

where

$$a_{mk} = c_2 h_{mk} \qquad (7)$$

and c_2 is a scaling constant. Inspection of Eq. (6) shows that there is now a one-to-one correspondence between each element of the mask and the corresponding element of the matrix operator [H] in Eq. (3).

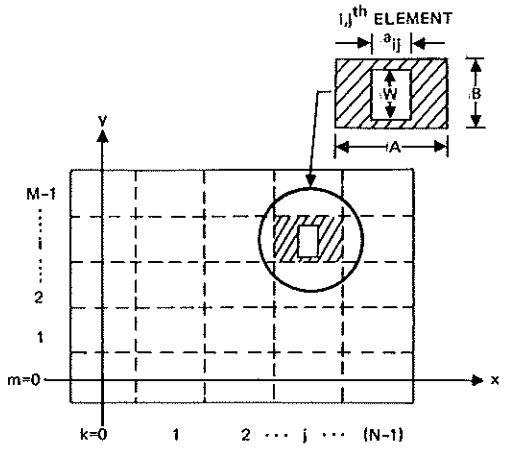

Fig. 4. Optical memory mask showing only i, j^{th} element. Mask consists of M x N rectangular elements, the clear portion of each having the same width W but a variable length a_{mk}.

The light field emerging from the optical mask is simply the product of the incident irradiance and the mask transmittance function. The resulting light distribution is then imaged onto the plane of the detector via a scanning mirror. The irradiance distribution in the x', y' plane resulting from the temporally modulated mask image, moving at a speed v in the negative x' direction, is then

$$E'(x',y';t) = c_3 E(t)\tau\left(\frac{x'+vt-x'_o}{\beta},\frac{y'}{\beta}\right) \tag{8}$$

In this equation c_3 is a constant determined from radiometric considerations of the imaging system, x'_o is an arbitrary spatial phase term associated with the scanning, and β is the lateral magnification associated with the mapping of the optical mask into its image.

Knowing the irradiance distribution in the detector plane, the quantity of interest in terms of the response of the CCD is the total exposure delivered to the x',y' plane during a single sweep of the mirror. This is given by

$$\xi(x',y') = \int_0^\infty E'(x',y';t)dt. \tag{9}$$

Making the appropriate substitutions from Eq. (4) through (8), the total exposure becomes

$$\xi(x',y') = c_1 c_3 \sum_{n=0}^{N-1}\sum_{m=0}^{M-1}\sum_{k=0}^{N-1} f_n \,\mathrm{rect}\left(\frac{y'-mB'}{W'}\right) \int_0^\infty \mathrm{rect}\left[\frac{t-(nT+d/2)}{d}\right]\mathrm{rect}\left[\frac{t-(kA'/v+x_o/v)+x'/v}{a'_{mk}/v}\right]dt \tag{10}$$

where for convenience we have defined the magnification-scaled quantities

$$A' = \beta A$$
$$B' = \beta B$$
$$W' = \beta W$$
$$a'_{mk} = \beta a_{mk}$$

Evaluating the integral in Eq. (10) we find that the m,k^{th} exposure element due to the n^{th} LED pulse is one of three possible trapezoidal solids.*

$$\xi(x',y')_{nmk} = \begin{cases} c_1 c_3 d f_n \mathrm{rect}\left(\frac{y'-mB'}{W'}\right)\mathrm{trap}\left[\frac{x'-(k-n)A'}{\frac{a'_{mk}-vd}{2},\frac{a'_{mk}+vd}{2}}\right] & a'_{mk} > vd. \quad (11a) \\ \frac{c_1 c_3}{v} f_n a'_{mk}\mathrm{rect}\left(\frac{y'-mB'}{W'}\right)\mathrm{tri}\left[\frac{x'-(k-n)A'}{a'_{mk}}\right] & a'_{mk} = vd. \quad (11b) \\ \frac{c_1 c_3}{v} f_n a'_{mk}\mathrm{rect}\left(\frac{y'-mB'}{W'}\right)\mathrm{trap}\left[\frac{x'-(k-n)A'}{\frac{vd-a'_{mk}}{2},\frac{vd+a'_{mk}}{2}}\right] & a'_{mk} < vd. \quad (11c) \end{cases}$$

In arriving at the expressions of Eq. (11), several important requirements have been included. First, it is assumed that the moving mask image is in phase synchronization with the LED such that the first (k=0) column of the mask image is centered on the y'-axis half way through the first (n=0) LED pulse. This implies that

$$x'_o = \frac{vd}{2}.$$

Second, the timing of the LED pulses must be such that the exposure pattern will be of the proper scale. That is, it will ensure that half way through the n^{th} light pulse the k=n^{th} column of the mask image will also be centered on the y'-axis. This means that

$$A' = vT.$$

*See Appendix A for definitions of the rect, trap, and tri functions used here. Also see Appendix B for evaluation of the form of integral contained in Eq. (10).

The exposure elements described by Eq. (11) and their size relationships to a CCD element are illustrated in Fig. 5. The exposure element $\xi(x',y')_{nmk}$ describes the distribution of radiant energy per unit area delivered to the detector plane from the m,kth mask element during the nth LED pulse. As can be seen from the diagram, the size of a given exposure element relative to the size of a CCD element must be considered when computing the total radiant energy actually entering the CCD element. Of the five possible combinations described in Fig. 5, three pass an amount of radiant energy during a single light pulse which is proportional to the desired product $f_n a'_{mk}$. These are cases (a) and (b) with trapezoid height $R = (c_1 c_3/v) f_n a'_{mk}$ and case (b) with $R = c_1 c_3 d f_n$. Of these three we select the first for practical consideration since it greatly reduces tolerance requirements in mask fabrication and in scan synchronization. Therefore, combining Eq. (10) and (11c), the total exposure in the x',y' plane is

$$\xi(x',y') = \frac{c_1 c_3}{v} \sum_{n=0}^{N-1} \left\{ \sum_{m=0}^{M-1} \sum_{k=0}^{N-1} f_n a'_{mk} \right. \qquad (12)$$
$$\left. \text{rect}\left(\frac{y'-mB'}{W'}\right) \text{trap}\left[\frac{x'-(k-n)A'}{\frac{vd-a'_{mk}}{2}; \frac{vd+a'_{mk}}{2}}\right] \right\}$$

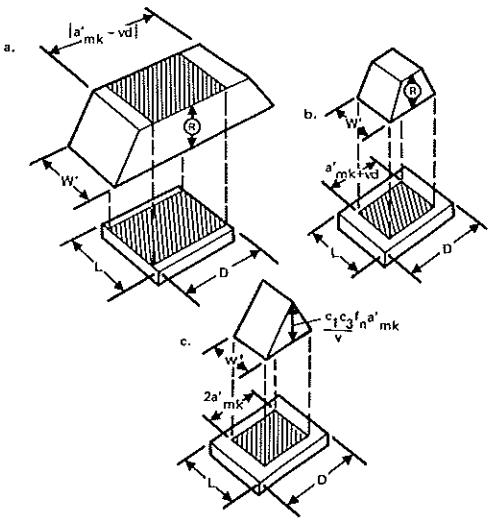

Fig. 5. Possible relationships between exposure element and detector element as described by Eq. (11). Eq. (11a) can correspond to cases (a) or (b) above where $R = c_1 c_3 d f_n$. Eq. (11b) is represented by case (c) above, and Eq. (11c) is described by cases (a) or (b) with $R = c_1 c_3/v\, f_n a'_{mk}$.

As shown in Fig. 6, the expression in braces, $\{\ \}$, above, represents a rectangular array of trapezoidal solids due to the nth LED pulse. A new such exposure array is created with each input pulse f_n, but each array is shifted from the preceding by an amount A'. Note from the figure that for the nth input light pulse, only the k=nth column of the exposure array will be superimposed upon the detector. Finally, we assume that in the y'-dimension, each exposure element is narrower than a CCD element. In summary, the assumptions

$$k = n$$
$$L \geqslant W'$$
$$D \leqslant vd - a'_{mn},$$

when combined with Eq. (12), yield the total radiant energy entering the mth CCD element during a complete mirror sweep as

$$Q_m = c_1 c_2 c_3 \frac{LD}{v} \sum_{n=0}^{N-1} f_n h_{mn}. \qquad (13)$$

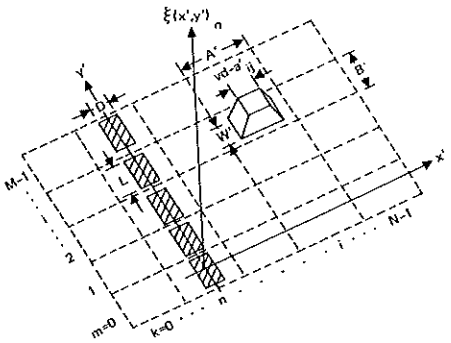

Fig. 6. Exposure pattern $\xi(x',y')_n$ due to the nth LED pulse. Pattern is rectangular array of trapezoidal solids (only i,jth exposure element shown) shifted in the negative x' direction by an amount nA'. Note that nth column of exposure array is centered on the detector array (shaded elements).

Comparison of Eq. (13) with Eq. (2) shows that the quantity Q_m is indeed proportional to the desired quantity g_m. At the completion of a given mirror sweep the charge packets stored in each of the M CCD elements are clocked sequentially out of the device yielding a time sequence of pulses which are respectively proportional to the elements of the desired column vector [G] in Eq. (3).*

*The assumption is that the energy entering each CCD element is linearly converted to charge within the element. Deviations from this assumption, or compensation techniques, will not be discussed in this paper.

One final consideration is the relation between the length of the mask elements, a_{mk}, and their spacing in the x-dimension. A profile of the m,n^{th} trapezoid function of Eq. (12) is shown in Fig. 7, where it is superimposed upon the m^{th} CCD element of width D.

For a given pulse duration d and velocity v, note from the figure that, while the scope of the trapezoid sides depends upon the LED pulse strength f_n, the overall width of the exposure element depends solely upon the length of the mask image element a'_{mn}. Also notice that the upper vertices of the trapezoid lie on the legs of a triangle shown by dashed lines. Thus, for a given f_n, the top of the trapezoid gets higher and narrower as a'_{mn} increases. Since the detector must lie within the flat portion of the exposure element, a'_{mn} can vary between zero and a maximum value determined by the CCD element width D. In terms of the mask element itself,

$$0 \leqslant a_{mn} \leqslant \frac{vd - d}{\beta} . \qquad (14)$$

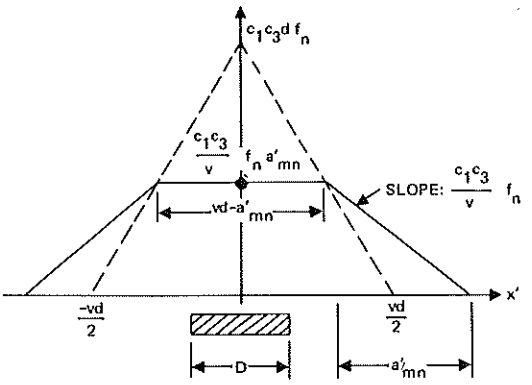

Fig. 7. Profile of m,n^{th} exposure element superimposed upon m^{th} CCD element (shaded). Uper vertices of trapezoid always lie on legs of triangle shown with dashed lines.

To calculate the minimum spacing required between mask elements, the overlap between two adjacent trapezoidal elements for which a'_{mn} is a maximum must be considered. As shown in Fig. 8, the minimum allowable spacing in the exposure plane then occurs when d=T. From the figure we conclude that the absolute minimum spacing of mask elements must therefore be

$$A_{min} = \frac{vT}{\beta} . \qquad (15)$$

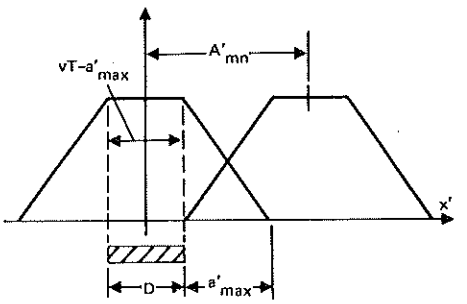

Fig. 8. Minimum possible spacing between adjacent exposure elements occurs when d = T and when a'_{mn} assumes the maximum value $a'_{max} = vT - D$.

AREA-ARRAY PROCESSOR

GENERAL DESCRIPTION

In the system described below, the need for a scanning mirror is eliminated by incorporating an area-array detector in place of the line-array CCD used above. By using a two-dimensional CCD, the scanning of the mask image can now be performed electronically within the detector itself. This allows considerable simplification in system design as well as analysis. Such a modified system is represented in Fig. 9, where up to the optical memory mask the geometry is essentially the same as in the line-array system described by Fig. 2. Immediately behind the mask is an area-array CCD whose output is a sequence of pulses representing the desired vector [G]. This geometry not only avoids the mechanical complexity of a scanning mirror, but also eliminates the imaging lens and the space associated with its mapping of the mask image onto the detector.*

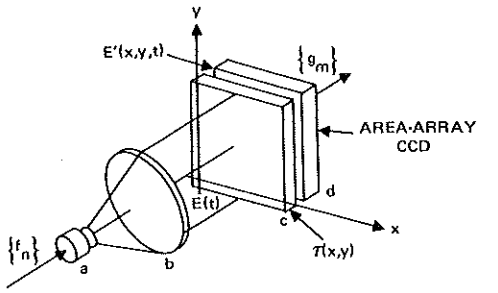

Fig. 9. Area-array electrooptical processor in which need for a scanning mirror is eliminated through use of a two-dimensional CCD. System consists of: (a) LED; (b) condensing lens; (c) optical memory mask; and (d) area-array CCD.

*We speak here of the mask and detector as being in physical contact, as indeed they could be with a specially designed CCD. However, for convenience in the experimental work performed thus far, the mask has been imaged onto the detector with a lens.

MATHEMATICAL ANALYSIS

As before, we represent the spatially uniform light field incident upon the optical mask by

$$E(t) = c_1 \sum_{n=0}^{N-1} f_n \, \text{rect}\left(\frac{t-nT-d/2}{d}\right) \tag{16}$$

where c_1 is a constant scale factor.

For ease of fabrication, we again represent the elements of the optical mask as a rectangular clear apertures arranged on a rectangular array with spacing A x B (Fig. 10). Here the clear portion of the m,kth mask element is of length $\sqrt{a_{mk}}$ in the x-dimension and width $K\sqrt{a_{mk}}$ in the y-dimension where

$$a_{mk} = c_2 h_{mk}, \tag{17}$$

$$K = B/A, \tag{18}$$

and c_2 is a scaling constant.

The transmittance function of the mask is then

$$\tau(x,y) = \sum_{m=0}^{M-1} \sum_{k=0}^{N-1} \text{rect}\left(\frac{x-kA}{\sqrt{a_{mk}}}\right) \text{rect}\left(\frac{y-mB}{K\sqrt{a_{mk}}}\right) \tag{19}$$

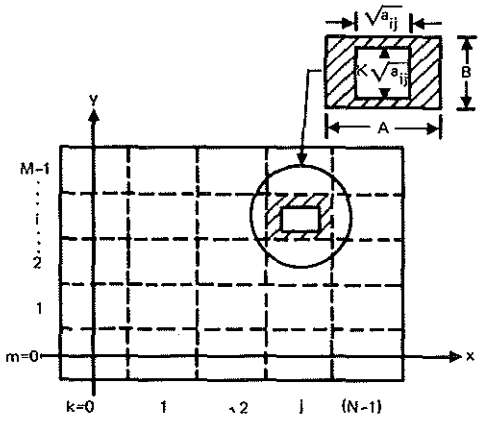

Fig. 10. Optical memory mask showing only i,jth element. Mask consists of rectangular array of M x N rectangular elements. The clear area of the i,jth element is Ka_{ij}, where K = B/A.

Immediately behind the optical mask the irradiance distribution incident on the detector plane is

$$E'(x,y;t) = E(t)\tau(x,y). \tag{20}$$

The optically sensitive region of the area-array CCD consists of a rectangular array of identical rectangular photosensors, as shown in Fig. 11. These CCD elements, each of size D x L, are arranged on an array the same size and scale as the optical mask. In addition, the aspect ratio of each mask element is scaled to be the same as that of the corresponding CCD element. That is,

$$\frac{B}{A} = \frac{L}{D} = K. \tag{21}$$

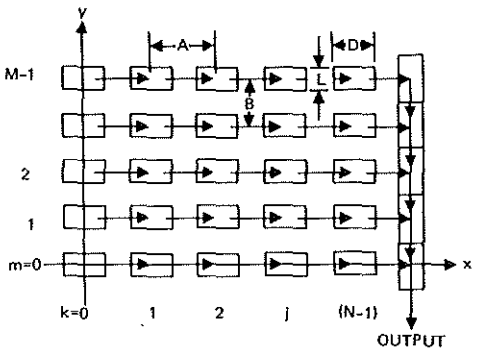

Fig. 11. Rectangular array of rectangular CCD photosensors. Each element is of size D x L, where L/D = B/A = K. Column at right represents output shift register for clocking out charge transferred from the photosensor array.

We now focus attention on the energy entering the m,kth element of the CCD due to the nth LED pulse,

$$Q_{nmk} = \int_{-\infty}^{\infty}\int\int E'(x,y;t)\,dx\,dy\,dt$$

$$= c_1 c_2 dK f_n h_{mk}. \tag{22}$$

In particular, the energy entering the k = nth element in the mth row is proportional to $f_n h_{mn}$, the product inside the summation of Eq. (2). What is desired is the sum of such products for all values of n. Thus, if the charge content of each CCD cell in the mth row is transferred laterally, as indicated in Fig 11, by one element between LED pulses, then the stored photocharge in the m,kth element due to the nth pulse can be added to the charge stored in the (m,k-1)st element due to the (n-1)st pulse. This means that the partial sum in the last (k=N-1) cell of the mth row after the rth pulse is

$$S_{mr} = c_1 c_2 dK \sum_{n=0}^{r} f_n h_{m,N-(r-n+1)} \qquad (23)$$

Finally, after the last pulse (r=N-1), the charge stored in the last cell of the m^{th} row is proportional to

$$S_{m,N-1} = c_1 c_2 dK \sum_{n=0}^{N-1} f_n h_{mn}. \qquad (24)$$

Again referring to Eq. (2), this expression is proportional to the desired quantity g_m. After N light pulses, the charge stored in the output shift register is vertically clocked out. This charge, in the form of discrete packets, yields a time sequence of pulses proportional to the values g_m of the desired column vector [G].

COMMENTS AND CONCLUSIONS

Eq. (13) and (24) predict that the line-array and area-array systems described above are capable of performing the linear transformation of Eq. (2). A developmental model of the line array processor, shown in Fig. 12, has been assembled and tested. The system is similar to that previously reported,[4-6] however, here a 500-element Fairchild line-array CCD has replaced the vidicon tube. In addition, a compact layout has been used in which the optical system is confined to a 4 x 5 inch circuit board.

An area-array processor which utilizes a 100 x 100 element Fairchild CCD has also been assembled, see Figure 13, and is currently being tested. The detector, which is a standard imaging chip, is being driven in a manner to suit this signal processing application. Used as an image sensor, the CCD array would continuously integrate during each full video frame.* However, for the case at hand the device integrates during each individual LED pulse, but between pulses the charge collected at each photosite is transferred laterally by one element and added to the photocharge from the next pulse. This shift-and-add process is repeated 100 times, after which the charge deposited in the output shift register, representing the desired output data vector, is clocked out.

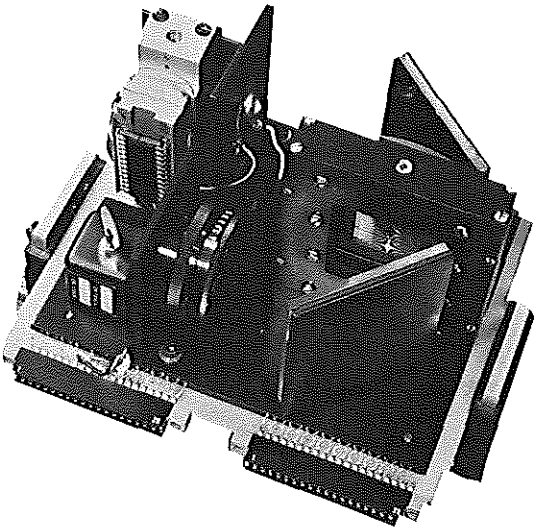

Fig. 12. Line-array electrooptical processor on a 4 x 5 inch circuit card. Device is programmable by inserting a desired program mask. Support electronics occupies three additional cards of the same size.

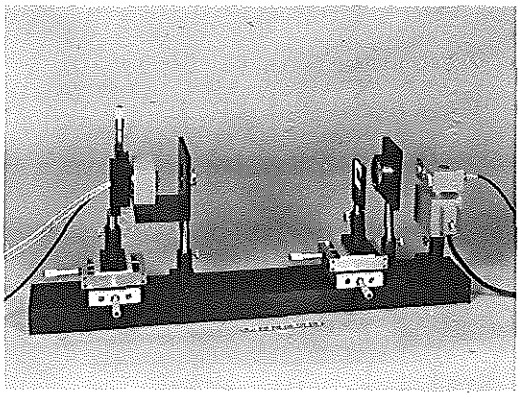

Fig. 13. Area-array electrooptical processor. Device is programmable by inserting desired program mask.

As described earlier, the optical memory masks fabricated thus far utilize an area modulation scheme for encoding the values h_{mn}. This technique is straightforward, not involving materials problems (e.g., nonlinearities), and lends itself to mask fabrication with a programmable desk calculator and x-y plotter. Two mask examples are shown in Fig. 14 for the cases of a discrete identity transform and a discrete cosine transform.

*Interlacing is ignored in this discussion.

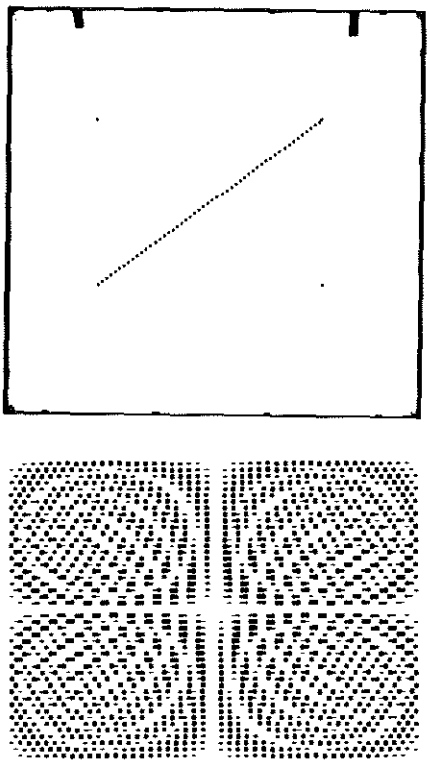

Fig. 14. Examples of 35 mm format memory masks designed to perform (a) a discrete identity transform, and (b) a discrete cosine transform.

These masks have been used in preliminary tests of the area-array processor, with favorable results illustrated in Figs. (15) and (16). As a first test we consider the case where the impulse response operator of Eq. (2) is a matrix with diagonal elements of unity and off-diagonal elements zero. This defines the so-called identity matrix. Its use in Eq. (2) reproduces at the output an exact replica of the input function. Typical performance of the area-array processor with an identity matrix in place is shown in Figure 15. In this example the input signal (lower trace) was a one volt (peak-to-peak) triangle wave of 0.8 kHz frequency, sampled at 10 kHz. As seen in the figure, the output signal (upper trace) is a well formed triangle wave of the same frequency as the input signal. The few spurious samples at each end of the output trace are not part of the processed signal and are ignored. As a second test, a mask was prepared for performing a discrete cosine transform. Theoretically, a pure cosine wave input results in two delta functions at the output, centered in the output array, and separated by a distance proportional to twice the input frequency. The results of this test are shown in Fig. 16 for two input cosine waves of one volt (peak-to-peak) amplitude and frequencies (a) 1.1 kHz and (b) 2.5 kHz. As can be seen from the figure, these results agree quite well within the theoretically predicted outputs.

It is appropriate at this point to consider the data rates associated with these processors. In the 500 x 1 line-array system of Fig. 12, a rather slow scanning mirror was used rather than a high speed spinning prism to demonstrate the concept. The data must be emptied out of the CCD at the end of each mirror scan before a new scan can begin. The time required to perform the transform on the next set of input samples is determined by the 20 msec sweep period of the mirror. In this system, input samples can be fed in at a continuous rate of about 1 kHz. The resulting output comes in 0.5 msec bursts of 500 data pulses at 1 MHz with 20 msec between bursts.

For the 100 x 100 area-array processor, the data can also be clocked from the output shift register at 1 MHz. This must be 100 times faster than the rate at which charge is being transferred across the array. Since for each lateral data shift there is one light pulse, a continuous input rate of 10 kHz yields a continuous output pulse rate of 1 MHz.

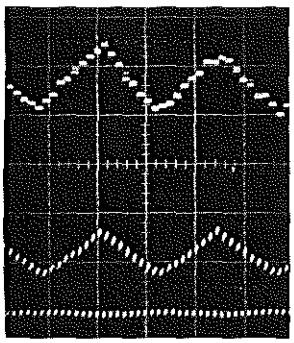

Figure 15. Input (lower trace) vs. output (upper trace) with identity matrix programmed into electrooptical processor.

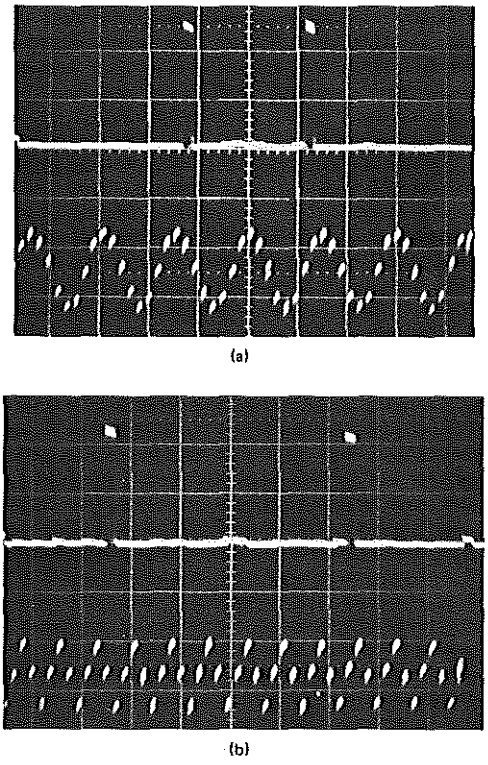

Figure 16. Input (lower trace) vs. output (upper trace) with processor programmed for a cosine transform. Input signals are cosine waves with frequencies (a) 1.1 kHz and (b) 2.5 kHz.

In performing a linear transformation, the line-array device operates on sequential windows of input data as shown in Fig. 17a. Although the output data appear in high-frequency bursts, over the period of one mirror cycle there are 500 output data pulses for each 500 input samples. However, in this area-array processor example there are 100 output data pulses for each input sample. What this means is that a new and complete transform is computed, with each input pulse, on a sliding window of input data (Fig. 17b). That is, each new set of output pulses represents the linear transformation of an input data set which differs from the preceding set by the addition of a new sample and the dropping of the oldest. If the functional form of the input signal varies in time, then its transform as a function of time can be continuously computed. This represents a useful capability inherently available in the device if required. An example of its use would be the computation of the discrete Fourier transform of a signal whose exact time of arrival is not known. Thus, one could avoid truncating the input signal by not including it entirely within the sampling window.

As a final comment, let us point out that although we have considered the analog input f(t) to have been sampled before modulating the LED, this is not in general necessary. When the input signal is sampled according to Eq. (4), the total light collected by a given CCD element due to the n^{th} LED pulse is exactly proportional to f_n. However, if the analog input is not sampled beforehand, then the "sampling" is done in effect by the CCD itself. The photosensitive elements of the CCD integrate the light incident upon them only during a time determined by the length of a photogate clocking pulse. This performs a sampling operation. However, the light integrated will be proportional to the average value of f(t) during the sampling interval. This average value will in most cases be sufficiently close to the instantaneous value f_n so that sampling of the input signal and all the associated synchronization problems can be eliminated.

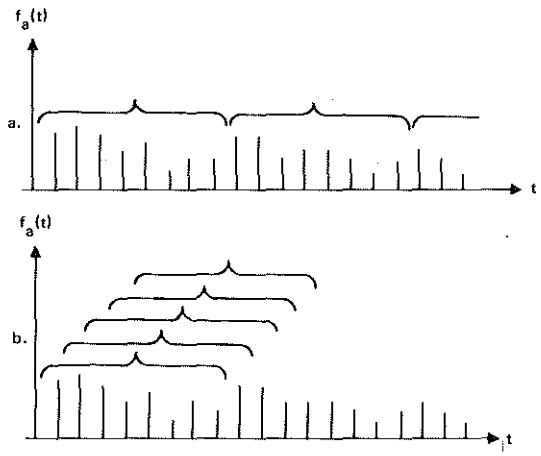

Fig. 17. With the area-array processor, transforms can be performed not only on (a) sequential windows of data but also on (b) input data under a sliding window.

ACKNOWLEDGMENT

This ongoing work is sponsored by the Naval Electronic Systems Command.

REFERENCES

1. R. A. Heinz, J. O. Artman, and S. H. Lee, Appl. Opt., 9,2161 (1970).
2. D. P. Jablonowski, R. A. Heinz, and J. O. Artman, Appl. Opt., 11,174 (1972).
3. L. J. Cutrona, Optical and Electro-Optical Information Processing, J. T. Tippet et al., Eds. (MIT Press, Cambridge, 1965), p. 97-98.

4. R. P. Bocker, Applied Optics, 13, 1670 (1974).

5. K. Bromley, Optica Acta, 21, 35 (1974).

6. R. P. Bocker, Ph.D. Dissertation, University of Arizona, June 1975.

7. R. P. Bocker, K. Bromley, and M. A. Monahan, "Optical Data Processing for Fleet Applications," *Naval Research Reviews*, (Office of Naval Research, Arlington, VA), p. 44, May - June 1974.

8. M. A. Monahan, R. P. Bocker, K. Bromley, and A. Louie, "Incoherent Electrooptical Processing with CCDs," *International Optical Computing Conference April 23-25, 1975, Digest of Papers*, (IEEE Catalog No. 75 CH0941-5C), p. 25

APPENDIX A

Many useful and often common functions must be defined in piecewise fashion because of abrupt changes in the value of the function. For example, consider the function f(u) such that

$$f(u) = \begin{cases} 0, & u < -a, \\ \frac{u}{a} + 1 & -a \leqslant u \leqslant 0, \\ -\frac{u}{a} + 1, & 0 \leqslant u \leqslant a, \\ 0, & u > a. \end{cases}$$

To achieve compactness and clarity of notation for such simple but awkwardly expressed functions, we define in Fig. A1 a set of functions which implicitly include such abrupt behavior. We refer to these as the rectangle, triangle, and trapezoid functions, respectively. Note that the piecewise function cited in the above example now may be simply written as

$$f(u) = \text{tri}\left(\frac{u}{a}\right).$$

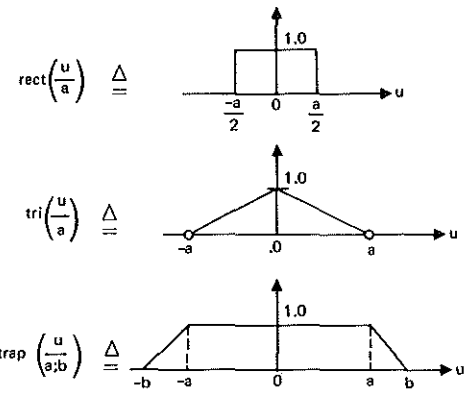

Fig. A1. Calculations involving abruptly changing functions are greatly simplified by adopting a compact notation. Used in this paper are three such awkwardly expressed functions which are simply defined as the (a) rectangle (rect), (b) triangle (tri), and (c) trapezoid (trap) functions, respectively.

APPENDIX B

The integral contained in Eq. (10) is of the form

$$\int_{-\infty}^{\infty} \text{rect}\left(\frac{u}{a}\right) \text{rect}\left(\frac{u \pm v}{b}\right) du. \qquad \text{(B1)}$$

The integrand in Eq. (B1) gives the area common to both rectangle functions when the second is offset from the first by an amount v (Fig. B1). Thus, the overlap area, which varies as a function of v, provides three possible solutions to the integral:

$$a \text{ trap}\left[\frac{v}{\left(\frac{b-a}{2}\right); \left(\frac{b+a}{2}\right)}\right], \quad a < b. \qquad \text{(B2a)}$$

$$b \text{ tri}\left(\frac{v}{b}\right), \quad a = b, \qquad \text{(B2b)}$$

$$b \text{ trap}\left[\frac{v}{\left(\frac{a-b}{2}\right); \left(\frac{a+b}{2}\right)}\right], \quad a > b. \qquad \text{(B2c)}$$

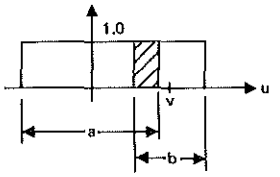

Fig. B1. Shaded overlap area between two rect functions gives value of integral in Eq. (B1) as function of displacement v.